Blue-green single-frequency laser based on the intracavity SHG of a diode-pumped Ytterbium-doped laser

Mathieu Jacquemet, Frédéric Druon, François Balembois, Patrick Georges

Blue-green single-frequency laser based on intracavity frequency doubling of a diode-pumped Ytterbium-doped laser

Mathieu Jacquemet, Frédéric Druon, François Balembois, Patrick Georges

Laboratoire Charles Fabry de l'Institut d'Optique, UMR 8501, Centre Universitaire, Bât. 503, 91403 Orsay Cedex, France.
mathieu.jacquemet@iota.u-psud.fr

Bernard Ferrand

LETI/DOPT/CEA-Grenoble 17, Rue des Martyrs, 38054 Grenoble Cedex 9, France.

Abstract: Single-frequency lasers in the blue-green (500 nm) visible spectrum are important for many applications including iodine precision spectroscopy, optical frequency standards or ionized argon lasers substitution. To the best of our knowledge, we report in this paper the first single-frequency diode-pumped Ytterbium-doped solid-state laser operating at 501.7 nm by intracavity second harmonic generation (SHG). The single-frequency fundamental infrared laser light is generated by a diode-pumped $Yb^{3+}:Y_2SiO_5$ crystal in a ring oscillator. Intracavity SHG with a $KNbO_3$ nonlinear crystal produced more than 50 mW of single-frequency blue-green radiation.

OCIS codes: (140.3480) Lasers, diode-pumped; (140.3560) Lasers, Ring; (140.3570) Lasers, Single-mode; (140.3580) Lasers, Solid-State; (140.7300) Visible Lasers; (190.2620) Frequency conversion.

References and Links

1. S. Picard, L. Robertson, L.-S. Ma, K. Nyholm, M. Merimaa, T.E. Ahola, P. Kren, and J.-P. Wallerand, "Comparison of $^{127}I_2$-satbilized frequency-doubled Nd:YAG lasers at the Bureau International des Poids et Mesures," Appl. Opt. **42**, 1019-1027 (2003).
2. W.-Y. Cheng, L. Chen, T.H. Yoon, J.L. Hall, J. Ye," Sub-Doppler molecular-iodine transitions near the dissociation limit (523–498 nm)," Opt. Lett. **27**, 571-573 (2002).
3. J.-C. Keller, M. Broyer, and J.-C. Lehmann, "Mesure directe de la durée de vie et des facteurs de Landé du niveau $^3\pi_{O+}$, ν'=62, J'=27 de la molécule I_2," C.R Acad. Sc. Paris tome 277-série B, 369-372 (8 octobre 1973).
4. J. Ye, L-S Ma, and J. L. Hall, "High resolution frequency standard at 1030 nm for Yb:YAG solid-state lasers," J. Opt. Soc. Am. B **17**, 927-931 (2000).
5. R. H. Abram, K. S. Gardner, E. Riis, and A. I. Ferguson, "Narrow linewidth operation of a tunable optically pumped semiconductor laser," Opt. Express **12**, 5434-5439 (2004), http://www.opticsexpress.org/abstract.cfm?URI=OPEX-12-22-5434
6. L. D. DeLoach, S. A. Payne, L. L. Chase, L. K. Smith, W. L. Kway, W. F. Krupke, "Evaluation of absorption and emission properties of Yb^{3+} doped Crystals for laser applications," IEEE J. Quantum Electron. **29**, 1179-1191 (1993).
7. M. Jacquemet, F. Balembois, S. Chénais, F. Druon, P. Georges, R. Gaumé, and B. Ferrand, "First diode-pumped Yb-doped solid-state laser continuously tunable between 1000 and 1010 nm," Appl. Phys. B **78**, 13-18 (2004).
8. W. Drozdowski, A. J. Wojtowicz, D. Wisniewski, P. Szupryczynski, S. Janus, J. L. Lefaucheur, and Z. Goub, "VUV spectroscopy and low temperature thermoluminescence of LSO:Ce and YSO:Ce," J. Alloys and Comp. **380**, 146-150 (2004).
9. C. K. Chang, J.Y. Chang, and Y. K. Kuo, " Optical Performance of Cr:YSO Q-switched Cr:LiCAF and Cr:LiSAF Lasers," in *High-Power Lasers and Applications* Proc. SPIE **4914**, 498-509 (2002).

10. C. Deka, B. H. T. Chai, Y. Shimony, X. X. Zhang, E. Munin, and M. Bass, "Laser performance of Cr^{4+}:Y$_2$SiO$_5$," Appl. Phys. Lett. **61**, 2141-2143 (1992).
11. B. Comaskey, G. F. Albrecht, S. P. Velsko, and B. D. Moran, "24-W average power at 0.537 µm from an externally frequency-doubled Q-switched diode-pumped Nd:YOS laser oscillator," Appl. Opt. **33**, 6377-6382 (1994).
12. C. Li, R. Moncorgé, J.C. Souriau, C. Borel, and C. Wyon, "Room temperature CW laser action of Y$_2$SiO$_5$:Yb^{3+}, Er^{3+} at 1.57 µm," Opt. Commun. **107**, 61-64 (1994).
13. M. Jacquemet, C. Jacquemet, N. Janel, F. Druon, F. Balembois, P. Georges, J. Petit, B. Viana, D. Vivien, and B. Ferrand, "Efficient laser action of Yb:LSO and Yb:YSO oxyorthosilicates crystals under high-power diode-pumping," Appl. Phys. B **80**, 171-176 (2005).
14. S. Chénais, F. Balembois, F. Druon, G. Lucas-Leclin, and P. Georges, "Thermal lensing in diode-pumped ytterbium lasers - Part.I: Theoritical analysis and wavefront measurements," IEEE J. Quantum Electron. **40**, 1217-1233 (2004).

1. Introduction

Secondary optical frequency standards are of great interest for metrological applications, for high resolution spectroscopy, space-based measurements, or for fundamental tests in physics. The inherent frequency stability of solid-state lasers, due to low intrinsic noise level compared to dye or gas lasers, makes them very attractive for such laser sources. In addition, a solid-state laser can be compact, reliable, and long-lived. Blue-green hyperfine optical transitions in molecular iodine (^{127}I$_2$) are often used for laser stabilization and for the development of optical frequency standards, mainly at 532 nm [1]. Nevertheless, molecular iodine hyperfine transitions are numerous and narrow (<250 kHz) between 498 and 532 nm [2] but their natural linewidths become narrower when the wavelength is decreasing. In particular, hyperfine transitions around 501.7 nm seem to be very interesting because of their small natural linewidth around 11 kHz [3].

Since there is no optical transition at 501.7 nm in solid state materials, it is impossible to reach directly this blue-green wavelength. However, by frequency doubling a laser source operating around 1 µm, it is possible to reach such wavelength and to stabilize the laser radiation on one of these I$_2$ transition lines. Various choices can be done as for the diode-pumped laser medium around 1 µm, such as Yb or Nd-doped crystals, Yb-doped fibers or semiconductors. Among all, best promising solutions are certainly based on Ytterbium-doped crystals [4], because they exhibit more advantages compared to Neodymium doped crystals, as we will see later. Nevertheless, Optically Pumped Semiconductor (OPS) lasers could be another alternative way to reach this range of wavelength, as shown recently [5].

In this paper, we present a single-frequency laser emitting at 501.7 nm based on the intracavity second harmonic generation of a single-frequency diode-pumped Yb-doped laser emitting at 1003.4 nm. The Ytterbium doped crystal is pumped around 980 nm corresponding to the Zero-Line transition which is the stronger absorption line, between the fundamental level and the lowest level of the excited state manifold.

Usually, Ytterbium-doped bulk crystals exhibit weak absorption lines between 900 and 950 nm, a strong absorption peak around 980 nm (the Zero-Line transition), and emission transitions between 1010 and 1090 nm, which could be broad or narrow depending on the host matrix [6]. Many of them present high emission cross-sections between 1020 and 1060 nm, but only few have an important emission cross-section around 1.00 µm. One of them, Yb:Y$_2$SiO$_5$ (Yb:YSO), has been identified to be a well-adapted candidate since it combines a strong Zero-Line absorption at 978 nm and a high emission cross-section around 1003 nm [7].

Using the Zero-Line absorption transition presents many advantages. Firstly, it allows using commercially available high-power single-emitter InGaAs laser diode for the pump source. Secondly, it allows minimizing the quantum defect between the absorbed and emitted photons which reduces the heat deposition into the crystal. However, the choice of such a pumping wavelength involves two main constraints. First, the small difference between pump and laser wavelengths prevent the use of a standard dichroic mirror as the input mirror in case of a longitudinal pumping configuration. Indeed, such a mirror has to be highly transparent at

the pump wavelength (978 nm) and highly reflective at the laser wavelength (1003 nm) with high accuracy. Furthermore, the energy level scheme involved in this laser transition corresponds to a quasi-three levels one, really close to a "quasi-two levels" system. So, thermal population of the lower level of the laser transition is strong, leading to significant reabsorption at the emission wavelength. Thus, the pump absorption has to be highly saturated all along the crystal, in order to reduce the population of the lower level of the laser transition.

2. $Yb^{3+}:Y_2SiO_5$ properties

Oxyorthosilicates YSO (Y_2SiO_5) crystals have already been used in a large number of photonic applications, such as scintillators when doped with Cerium ions [8], saturable absorbers when doped with Chromium ions [9] or such as laser materials since it has previously been doped with Cr^{3+}, Nd^{3+}, $Er^{3+}:Yb^{3+}$, and Yb^{3+} ions [10-13]. Therefore, concerning the continuous-wave Ytterbium-world, Yb:YSO crystal has been used to provide a powerful widely tunable laser [13] as well as a finely tunable laser source between 1000 and 1010 nm [7], corresponding to the first step towards a single-frequency laser source at 1 µm.

Ytterbium-doped Yttrium oxyorthosilicate (Yb:YSO) is a monoclinic positive biaxial crystal, grown by the Czochralski process at the CEA-LETI (Grenoble, France). The sample was 1-mm long, anti-reflection coated around 1 µm and 5 at. % Yb-doped (9.2×10^{20} ions.cm^{-3}). It was cut with the Y axis along the propagation direction, corresponding to the b axis of the crystalline matrix, which is also the growth axis. Absorption and emission spectra of Yb:YSO along the available X and Z optical axes can be found in [13].

As previously written, this crystal exhibits a strong absorption line at 978 nm ($\approx 2.2 \times 10^{-24}$ m^2) on both available polarization axes. The 3.5 nm full-width at half-maximum (FWHM) of this transition is well-adapted for diode-pumping.

Without any intracavity wavelength selector, the quasi-three level nature of the transition leads to a laser oscillation at long wavelength depending on the crystal length and on the transmission of the output coupler. Typically, with a transmission of 4% for the output coupler and a 1 mm-long Yb:YSO crystal, free running laser oscillation occurred at 1042 nm, while the emitted wavelength was shifted towards 1082 nm for a 2 mm-long crystal. Therefore, we used a short crystal (thickness of 1 mm) and we had to insert spectrally variable losses into the cavity in order to prevent laser oscillation at long wavelengths (>1010 nm).

3. Experimental setup

We used the off-axis pumping scheme presented in [7], which allows overcoming problems induced by the quasi-three-level nature of the transitions. This pump source was a SDL laser diode producing a maximum power of 4 W around 980 nm from an emitting area of 1×100 µm^2. The pump beam was linearly polarized along the X-axis of the laser crystal. A spatial beam-shaping was used to reach a nearly square pump spot at the focus point of about 110×125 µm^2.

In order to obtain single-frequency laser oscillation, we used a ring "double bow tie" cavity as shown on Fig. 1. Taking into account the rectangular shape of the pump beam near the focusing doublet and in order to reduce the off-axis angle between the pump beam and the fundamental cavity mode, the input mirror was a rectangular slice of a classic concave mirror (R=100 mm-HR 1 µm). The pump beam was focused into the crystal above the input mirror M_1 as shown on Fig. 1. The crystal, inserted in a copper mount, was thermally regulated at 18°C via a Peltier cooler.

In order to highly saturate the population inversion and to reduce the reabsorption at the laser wavelength, we used a recycling device for the unabsorbed pump beam. This recycling device was simply composed of a lens (f = 145 mm) combined with a right-angle prism. The unabsorbed pump beam passed under the mirror M_2, was collimated by the lens, reflected by the prism and was finally refocused back into the crystal above the mirror M_2. The combination of the pump beam shaping and the recycling device has led to a high pump power density into the crystal (≈ 30 kW.cm^{-2} compared to 10 kW.cm^{-2} for the pump saturation intensity) and to decrease the reabsorption losses at the operating laser wavelength. The off-

axis pumping scheme allowed overcoming problems due to the small difference between the pump and the laser wavelengths. Using slices of mirrors reduced the off-axis pumping angle and increased the overlap between the pump and intracavity beams.
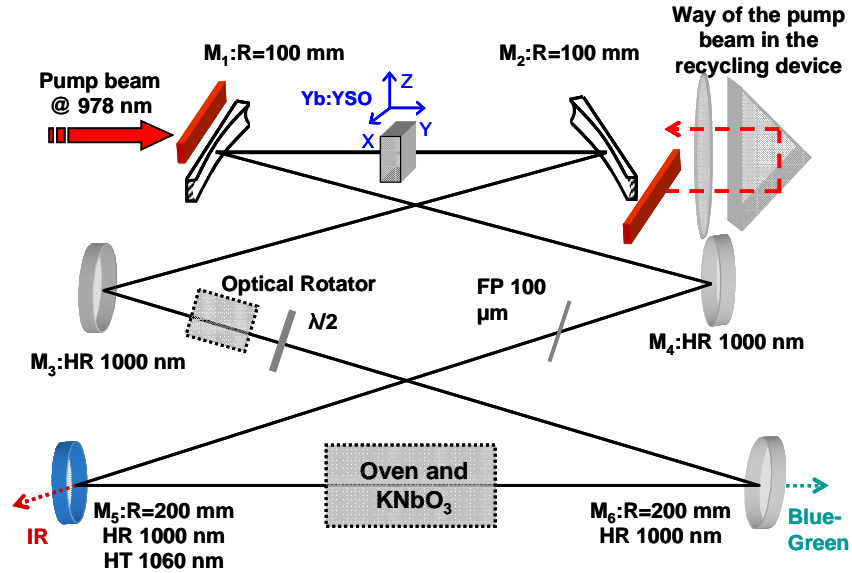

Fig. 1. "Double bow tie" cavity setup - M_1-$M_2 \approx 112$ mm, M_2-$M_3 \approx 230$ mm, M_3-$M_6 \approx 300$ mm, M_6-$M_5 \approx 245$ mm, M_5-$M_4 \approx 295$ mm, M_4-$M_1 \approx 235$ mm, FP:Fabry-Perot solid etalon.

The ring cavity was composed of 6 mirrors. It had been designed by taking into account the positive thermal lens induced by heat deposition into the crystal. Using the full study performed by Chenais *et al.* [14], we estimated the thermal focal lens in Yb:YSO to be around 100 mm for the maximum pump power and under lasing action. Nevertheless, in such a symmetrical ring cavity, the influence of the thermal lens on the stability range and on the cavity beam size is not really critical. Under these considerations, the first waist of the cavity between M_1 and M_2 was about 50 µm while the second one between M_5 and M_6 was around 80 µm and used for SHG. These values have been confirmed by experimental measurements. All the cavity mirrors, except the curved mirror M_5, were HR coated around 1 µm. The optical Faraday rotator and the half-wave plate, both AR coated around 1005 nm, maintained the unidirectional operation along *X*-axis polarization state where the gain is the highest. In that case, unstable single-frequency operation was obtained. A solid Fabry-Perot (FP) etalon (100 µm thickness of glass and uncoated) at Brewster angle acted as a polarizer and also allowed us to finely tune the laser wavelength. The free spectral range (FSR) of the ring cavity was about 210 MHz.

The key point of this resonator was the curved mirror M_5 which supported a special coating (HR 980 nm - HT 1064 nm) introducing losses at longer wavelengths (T>40% for λ>1025nm). Thus, the laser was forced to oscillate at shorter wavelengths around 1005 nm instead of 1042 nm in free running operation. Moreover, when tilted at about 5° like in our configuration, the transmission curve was shifted toward shorter wavelengths and the laser oscillated around 1003.5 nm. Finely tuning of the laser wavelength to 1003.4 nm was achieved by slightly tilting the solid Fabry-Perot etalon. However, in addition to prevent laser oscillation at higher wavelengths, M_5 also acted as an infrared output coupler for the resonator. Its transmission value has been measured to be only 0.5 % at 1003.4 nm.

Intracavity SHG was performed with a type I temperature-tuned non-critical quasi-phase-matching $KNbO_3$ crystal, placed inside an oven at 76.5 °C. The oven's dimensions (50 mm in diameter and 50 mm-long) imposed constraints on the cavity setup, which led to use a 200 mm radii of curvature for both mirrors M_5 and M_6. The nonlinear $KNbO_3$ crystal was *b*-cut,

9.5 mm-long, anti-reflection coated for both fundamental and second harmonic wavelengths. The fundamental optical wave, polarized along the *X*-axis of the laser crystal, was propagated into the *a-b* plane (*X-Z* plane) of the $KNbO_3$, while the second harmonic generated wave was polarized along the *c*-axis (*Z*-axis). The cavity had two output mirrors, M_5 for the infrared and M_6 for the second harmonic wavelength at 501.7 nm.

4. Experimental results

The available incident pump power on Yb:YSO laser crystal was 3.2 W. The saturated absorption of the pump for a single-pass of the pump beam and without laser effect was 38 %, leading to an absorption coefficient of 4.8 cm⁻¹.

Without inserting the FP etalon in the cavity, unstable single-frequency operation at 1003.4 nm and 501.7 nm was obtained. The insertion of the thin FP etalon at Brewster angle (in order to maintain the polarization along the *X*-axis) provided stable single-frequency operation at 1003.4 nm and 501.7 nm. Figure 2 represents the single-frequency output powers obtained simultaneously at 1003.4 nm and 501.7 nm versus the incident pump power at 978 nm.
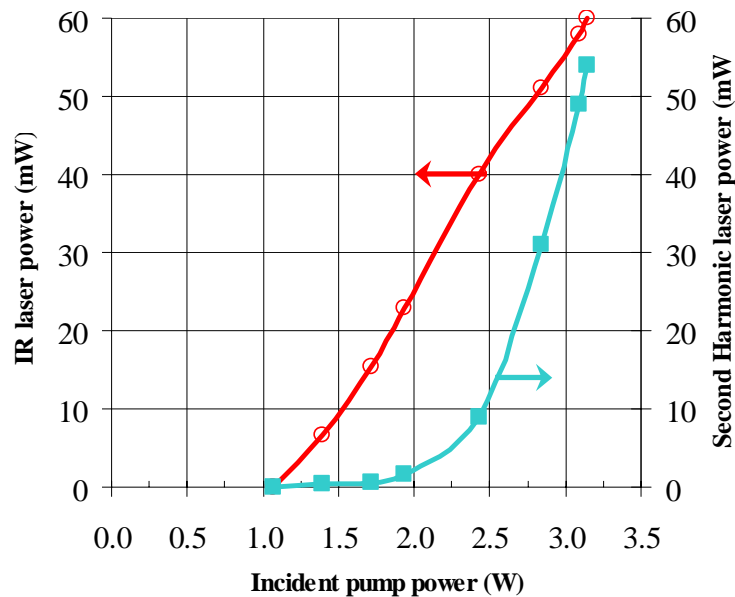

Fig. 2. Output powers at 1003.4 nm and 501.7 nm in single-frequency operation.

We have obtained simultaneously a cw power of 60 mW of single-frequency radiation in the IR and a cw power of 54 mW at 501.7 nm. The infrared intracavity power was estimated to be about 12 W leading to a SHG conversion efficiency of only 0.45 %. The overall optical to optical efficiency was 1.3 % for the blue-green wavelength. We can put forward three main facts. First, as already mentioned above, the intracavity power is limited by the transmission of folding mirror M_5. Secondly, the cavity waist involved in the SHG process was rather large (80 μm). Indeed, the oven's dimensions constrained us to use curved mirrors with 200 mm radii of curvature. Thirdly, the length of the $KNbO_3$ (9.5 mm) was not well optimized yet since the confocal parameter $\dfrac{2\pi n \omega^2}{\lambda_{IR}}$ was much larger (about 44 mm) than the crystal length, where n is the refractive index of $KNbO_3$ at λ_{IR} and ω is the radius of the cavity mode at the waist of the SHG process.

A 50 mm confocal scanning Fabry-Perot interferometer (FSR ≈ 1.5 GHz) was used to analyze the frequency spectrum of the fundamental infrared laser beam. A typical scanning

trace is shown on Fig. 3 presenting the single-frequency property of the laser. The inset is a zoom of one transmission peak of the Fabry-Perot analyser. An upper limit of the FHWM linewidth is deduced by comparison with the analyser FSR.
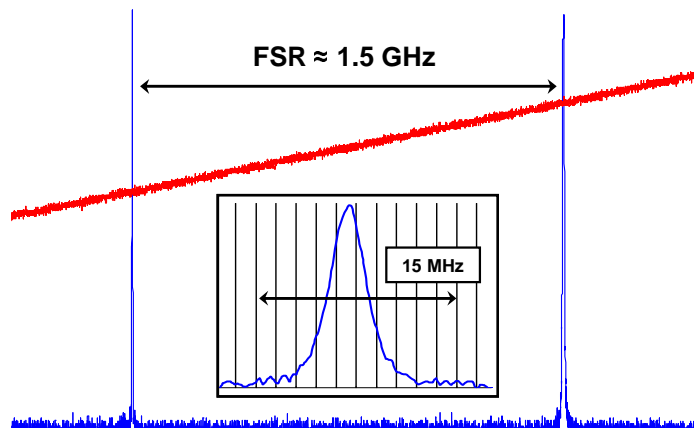

Fig. 3. Typical 1.5-GHz confocal scanning Fabry–Perot trace for the 1003.4 nm beam, confirming single-frequency operation. <u>Inset</u>: Zoom of one peak (1 graduation = 1.5 MHz)

We then deduced a linewidth of less than 3 MHz for the fundamental wavelength, limited by our detection system and depending on the alignments.

Although the single-frequency nature has only been measured on the fundamental laser beam (due to a lack of appropriate mirrors in the blue-green range), we naturally deduced that the second harmonic emission also exhibited single-frequency characteristic. Obviously, the M^2 parameter of the fundamental laser beam is equal to unity.

5. Conclusion and comments

In conclusion, we have presented in this paper the first diode-pumped single-frequency laser emitting simultaneously a power of 50 mW at 501.7 nm and 60 mW in the fundamental harmonic. This laser source is based on a diode-pumped Yb-doped crystal combined with intracavity SHG. Finally, we would like to highlight few points. Firstly, we have developed one of the lowest quantum defects (2.6%) diode-pumped lasers around 1 µm at room temperature. This has only been possible by the use of an off-axis pumping scheme combined with a high saturation of the pump absorption and also with the insertion of high losses at long wavelength to prevent their laser oscillation. Secondly, the pump source is a low-cost single emitter laser diode providing 4 W. We reached, in a direct diode-pumping scheme, a visible wavelength strongly interesting in a lot of research fields, such as fundamental physics, I_2 spectroscopy, or metrology. However, it is clear that the SHG stage was not optimized. Future prospects will be focused on the enhancement of the SHG efficiency and on the stabilization of the laser emission on an iodine hyperfine transition in order to reduce its linewidth and to reduce the long-term frequency drift of the laser.